3.2.3 SPA-limited and digitizer-limited spatial resolution

As a result of the serialization of the 2-D image by ADFT, only one dimension's spatial resolution, i.e. the *y*-direction, is subject to the effects of the SPA-limited and the digitizer-limited operation regimes. Similar to Eqs. (3) and (5), we can respectively write the SPA-limited (δy_{2D}^{SPA}) and digitizer-limited spatial resolution ($\delta y_{2D}^{\det}$) as,

$$\delta y_{2D}^{SPA} = C_y \cdot \delta\lambda_{SPA} \tag{13}$$

$$\delta y_{2D}^{\det} = C_y \cdot \delta\lambda_{\det}. \tag{14}$$

In contrast, the actual spatial resolution in the *x*-direction (δx_{2D}) does not depend on the properties of ADFT and the digitizer, and hence is only affected by the spatial-dispersion properties by the 2-D spatial disperser. Therefore,

$$\delta x_{2D} = \delta x_{2D}^{spatial}. \tag{15}$$

The dependence of actual spatial resolution in the *y*-direction (δy_{2D}) on GVD follows the similar trend shown in the 1-D case [compare Fig. 7(a) and 2(a)]. The system transits from digitizer-limited, SPA-limited to spatial-dispersion limited operation with increasing GVD. Same trend can also be observed in temporal resolution, which is given by $\delta t_{2D} = D \cdot \delta y_{2D} / C_y$ [Fig. 7(b)]. In this example, the 2-D STEAM system is preferable to operate at ~5 – 6ns/nm in order to make the temporal resolution of the system to be limited only by the available GVD while keeping the best achievable spatial resolution, i.e. δy_{2D} ~0.7 μm. It should be reminded such a large GVD can readily be made possible by the mean of optical amplification in STEAM, which overcomes the inherent loss associated with GVD. An extraordinarily large dispersion of > 10ns/nm has been demonstrated in ADFT-based spectroscopy with ultra-high spectral resolution [13].

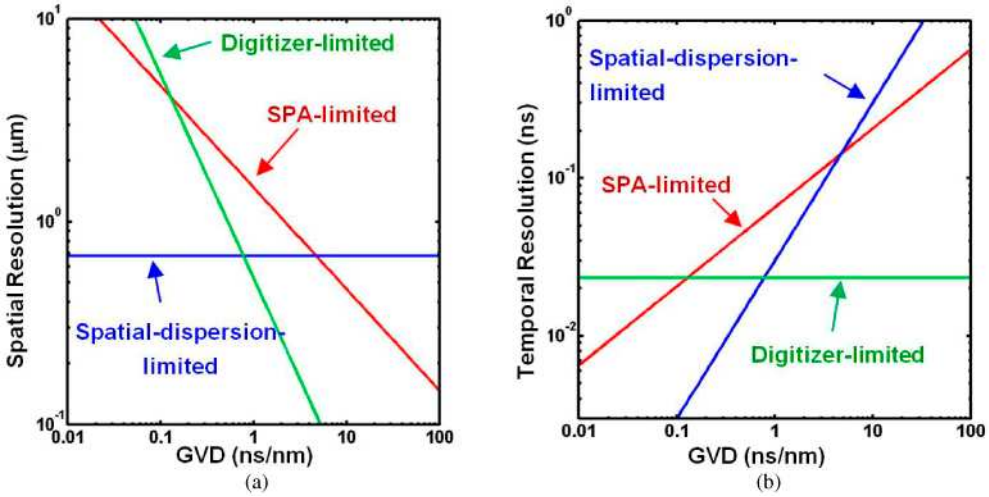

Fig. 7. (a) Spatial resolution of 2-D STEAM in the *y*-direction and (b) the corresponding temporal resolution in various limiting cases: digitizer-limited (green), SPA-limited (red) and spatial-dispersion-limited (blue), as a function of total GVD. The relevant system parameters are: a center wavelength of 800 nm, an objective lens with NA = 0.9 (f = 2 mm), a glass VIPA (n = 1.48) with tilt angle of 7°, thickness of 0.25 mm, $f_{\det}$ = 15 GHz.

4. Field-of-view, number of pixels and imaging frame rate

The field-of-view (FOV) of 1-D STEAM scales with the bandwidth of the spectral shower ($\Delta\lambda_{SS}$). Based on Eq. (2), the 1-D FOV is given by $\Delta x_{1D} = C_x \cdot \Delta\lambda_{SS}$. On the other hand, the

#125010 - $15.00 USD Received 4 Mar 2010; revised 23 Mar 2010; accepted 29 Mar 2010; published 28 Apr 2010

FOV of 2-D STEAM is set by spectral shower bandwidth and the FSR of the VIPA in the *x*- and *y*-direction, respectively. It can thus be estimated as $\Delta x_{2D} = C_x \cdot \Delta\lambda_{SS}$, and $\Delta y_{2D} = C_y \cdot \Delta\lambda_{FSR}$. Note that with the other parameters intact, the aspect ratio of the FOV can be tuned by varying $\Delta\lambda_{SS}$ and $\Delta\lambda_{FSR}$. Using the parameters shown in Fig. 5, we find Δy_{2D} ~80 μm which agrees well with the measurement [Fig. 5(a)], whereas Δx_{2D} ~200 μm with $\Delta\lambda_{SS}$ = 15 nm.

Another important parameter is the total number of pixels. It is equivalent to the number of data points sampled within each image-encoded temporal pulse after ADFT (i.e. single image frame). In 1-D STEAM, the temporal width of each pulse is set by spectral shower bandwidth ($\Delta\lambda_{SS}$) through ADFT, which is given by $\Delta\lambda_{SS} \cdot D$, the total number of pixels in 1-D STEAM (N_{1D}) can be written as

$$N_{1D} = \Delta\lambda_{SS} \cdot D \cdot f_{dig}, \tag{16}$$

where to f_{dig} is the sampling rate of the digitizer.

In 2-D STEAM, the numbers of pixels along the two orthogonal dimensions are defined in differently. In the *x*-direction, the number of pixels ($N_{2D\text{-}x}$) is essentially the number of columns in the spectral shower. In contrast, the number of pixels in the *y*-direction ($N_{2D\text{-}y}$) is the number of sampled point by the digitizer along each column of the spectral shower. Hence,

$$N_{2D-x} = \frac{\Delta\lambda_{SS}}{\Delta\lambda_{FSR}}, \tag{17}$$

$$N_{2D-y} = \Delta\lambda_{FSR} \cdot D \cdot f_{dig}. \tag{18}$$

Note that because of the serialization, only $N_{2D\text{-}y}$ depends on the GVD, and the sampling rate. The total number of pixels N_{2D} is thus given by,

$$N_{2D} = N_x \cdot N_y = \Delta\lambda_{SS} \cdot D \cdot f_{dig} \le \frac{f_{dig}}{f_{rep}}, \tag{19}$$

where f_{rep} is the repetition rate of the pulse laser, and hence is the frame rate of STEAM. From Eq. (19), we note that increasing GVD or the optical bandwidth can increase the frame length in time and hence the number of pixels. However, it comes at an expense of the laser repetition rate (i.e., the frame rate) in order to avoid the overlap between consecutive frames (i.e., $\Delta\lambda_{SS} \cdot D < f_{rep}^{-1}$). Fortunately, this limitation can be overcome by using a technique called virtual time gating, based on wavelength division multiplexing, to carve the single frame into multiple bands [23]. In such a parallel architecture, the number of pixels can be increased by the number of parallel channels (*M*) without sacrificing the frame rate (see Fig. 8),

$$N_{1D} = N_{2D} \le M \cdot f_{dig} / f_{rep}. \tag{20}$$

As shown in Eqs. (19) and (20), the number of pixels can be scaled up by increasing the optical bandwidth, GVD, the digitizer sampling rate and the number of parallel channels for implementing virtual time gating. For example, it is practical with today's technology to achieve ~300,000 pixels for a frame rate of 1 MHz using an optical bandwidth of ~150 nm, a dispersion of ~5 ns/nm, a digitizer sampling rate of 50 GS/s, using eight parallel virtual time gating channels (M = 8) (Fig. 8).

#125010 - $15.00 USD Received 4 Mar 2010; revised 23 Mar 2010; accepted 29 Mar 2010; published 28 Apr 2010

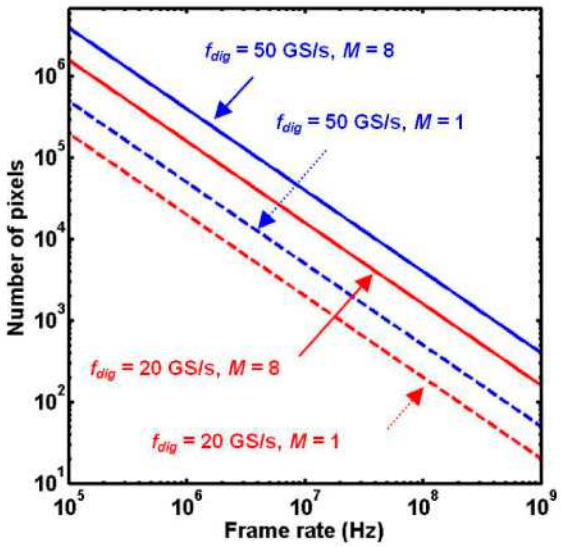

Fig. 8. Relationship between the number of pixels in STEAM and the frame rate based on Eq. (20). Note that it can be applied to both 1-D and 2-D STEAM. It is clear that the trade-off between the number of pixels and the frame rate can be overcome by employing virtual time gating with multiple channels (M = 8, solid lines).

5. Detection sensitivity

The detection sensitivity of STEAM is typically limited by a number of noise sources, namely the inherent shot noise of the input light (N_{shot}), the dark current noise (N_{dark}) and the thermal noise ($N_{thermal}$) of the photodetector. The shot noise is given by $N_{shot} = S_{in}^{1/2}$, where S_{in} is the number of signal photoelectrons collected by the photodetector. Consider an optical amplification process with a gain of G and a noise figure of F, the resultant shot noise at the photodetector becomes $G \cdot F \cdot N_{shot}$ [24]. Hence, the total noise of the system is

$$N_{total} = \sqrt{\left(G \cdot F \cdot N_{shot}\right)^2 + N_{dark}^{\ 2} + N_{thermal}^{\ 2}}. \tag{21}$$

Figure 9(a) shows the individual noise component in the system as a function of the number of signal photon per pixel, which is defined as Φ / f_{dig}, where Φ is the signal photon flux. For a system without gain (i.e. G = 1), it is shot-noise-limited when the signal photon number > ~1000. Decrease in signal photon number (< ~1000) however would turn the system into thermal-noise-limited ($N_{dark} << N_{thermal}$ at room temperature). In contrast, the system becomes shot-noise-limited in the presence of optical amplification. The merit of optical amplification becomes more apparent by investigating the SNR of the STEAM system. With an optically amplified signal, i.e. $G \cdot S_{in}$, the SNR is given by

$$SNR = \frac{G \cdot S_{in}}{N_{total}} = \frac{S_{in}}{\sqrt{\left(F \cdot \sqrt{S_{in}}\right)^2 + \left(\frac{N_{dark}}{G}\right)^2 + \left(\frac{N_{thermal}}{G}\right)^2}}, \tag{22}$$

where $S_{in} = \eta \cdot \Phi / f_{dig}$, where η is the quantum efficiency of the photodetector. Equation (22) shows that optical amplification effectively reduces both the dark current noise and the thermal noise by a factor of G, albeit the increase in shot noise by a factor of F. Hence, the SNR can be significantly enhanced if we implement the optical amplification with high gain and low noise-figure. Here, we employ distributed Raman amplification (DRA) within the dispersive fiber because DRA is well-known to have widely tunable and broadband gain spectrum, low noise figure, and the ability to maximize the SNR-to-distortion ratio by

#125010 - $15.00 USD Received 4 Mar 2010; revised 23 Mar 2010; accepted 29 Mar 2010; published 28 Apr 2010

keeping the signal power away from low power (noisy) and high power (nonlinear) regimes because of its distributed amplification nature [10–14].

The improvement in SNR as a result of optical amplification is depicted in Fig. 9(b). The optical amplification considerably enhances the SNR especially for the low light regime (i.e. < ~1000 photons per pixel) in which the system is originally thermal-noise-limited.

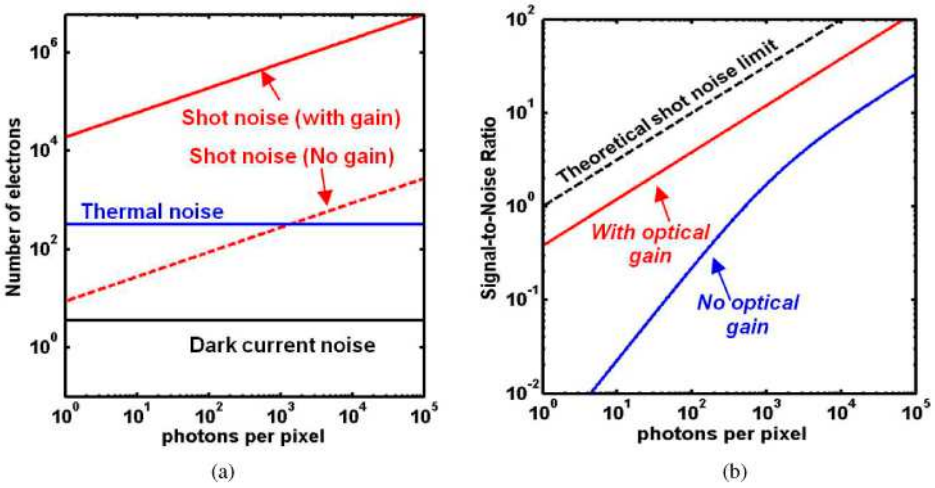

Fig. 9. (a) Noise components of STEAM: Dark current noise (black), thermal noise (blue), shot noise with gain, G = 30dB (red solid line) and shot noise without gain (red dashed line). (b) SNR of the system with gain, G = 30dB (red), and without gain (blue). The system parameters are: a photodetector with a bandwidth of 40 GHz, dark current of 100 nA, noise equivalent noise of 50pW/Hz$^{1/2}$ and η = 0.8. The f_{dig} = 50GS/s. the wavelength is 800 nm. Detailed calculation of N_{dark} and $N_{thermal}$ can be referred to Ref [24]. We assume DRA is employed within the dispersive fiber and a noise figure of ~3.5dB [25]. The dispersive fiber loss is assumed to be 20 dB. The black dashed line in (b) represents the theoretical shot noise limited SNR.

Furthermore, the system shows the minimum detectable number of signal photons is as low as ~7 for SNR = 1. It corresponds to an input referred noise of ~–150 dBm/Hz at λ = 800 nm. It should be emphasized again such detection sensitivity improvement enables the ultrafast imaging, on the order of MHz, in STEAM.

6. Concluding remarks

In conclusion, we have presented a model that quantifies the spatial and temporal resolution of the recently demonstrated STEAM imaging technology. We have also quantified the imager's detection sensitivity. We have shown that the spatial resolution is not simply governed by the diffraction limit, but it also depends on the spectral resolutions imposed by (1) the spatial disperser, (2) the amplified dispersive Fourier Transform (ADFT), and the digitizer's sampling speed and input bandwidth. We have also shown that there is a trade-off between the number of pixels and the frame rate as a consequence of the image serialization. However, this can be remedied by a technique known as virtual time gating; an all-optical time demultiplexer that enables parallel detection. This analysis not only provides valuable insight into this new imaging system, it also serves as a tool for design and optimization of STEAM imaging systems.

Real-time, continuous and ultrafast operation of STEAM naturally meets the demands of many high-speed imaging applications which involve detecting fast events that are very rare, rogue events. Both the 1-D and 2-D STEAM configurations can find a myriad of applications in these areas. 2-D STEAM in its native form could play a significant role in non-invasive high-speed reflectance confocal imaging, which has been employed in clinical applications, e.g. to monitor fast response to therapeutic treatment such as laser surgery [26, 27].

#125010 - $15.00 USD Received 4 Mar 2010; revised 23 Mar 2010; accepted 29 Mar 2010; published 28 Apr 2010

In contrast, having a simpler spatial disperser implementation and less stringent requirement on temporal dispersion (see Fig. 3 and 7), 1-D STEAM could find a compelling application in high-speed and sensitive imaging flow-cytometry [28]. In this case, the 1-D STEAM imager, operating in the line scan mode, is able to reconstruct the 2-D cross sectional images of the cells as they flow in the microfluidic channel at a high flow rate. Current flow cytometers have no means to offer real-time and high-speed imaging that matches the throughput of state-of-the-art flow cytometers (i.e. up to 100,000 cells per second [28]). This is mostly because of the lack of a camera technology with sufficient combination of speed and sensitivity. Combined with flow cytometry, 1-D STEAM provides an attractive means of delivering real-time imaging of cells and potentially performing screening of rare cancer cells such as circulating tumor cells [29].

Acknowledgements

This work was partially supported by the Defense Advanced Research Projects Agency (DARPA).

#125010 - $15.00 USD Received 4 Mar 2010; revised 23 Mar 2010; accepted 29 Mar 2010; published 28 Apr 2010